



4-Aminoacetophenone Intercalated CoAl Layered Double Hydroxides: Synthesis, Characterization and Adsorptive Removal of Cd(II) Ions from Water Samples

Abdul Rafay Bhatti¹, Ali Nawaz Siyal^{1*}, Qadeer Khan Panhwar¹,
Abdul Majid Channa¹, Muhammad Hassan Agheem²,
Adnan Ahmed³ and Muhammad Yar Khuhawar¹

¹Institute of Chemistry, University of Sindh, Jamshoro 76080, Pakistan.

²Centre for Pure & Applied Geology, Sindh, Jamshoro 76080, Pakistan.

³Centre for Environmental Science, University of Sindh, Jamshoro 76080, Pakistan.

*Corresponding Author Email: alinsiyal@usindh.edu.pk

Received 28 August 2020, Revised 25 March 2021, Accepted 26 March 2021

Abstract

In the present study, CoAl-NO₃ Layered Double Hydroxides (CoAl-NO₃-LDH) was synthesized and an enolate anion of 4-Aminoacetophenone (AAP) was intercalated into LDH following the reconstruction approach. The CoAl-NO₃-LDH and CoAl-AAP-LDH were characterized by Fourier-Transform infrared (FT-IR) spectroscopy, X-ray diffraction (XRD), scanning electron microscope (SEM) and energy dispersive X-ray (EDX) analyses. CoAl-AAP-LDH worked well for adsorption of Cd(II) ions from aqueous samples at optimum pH 7, adsorbent dosage 25 mg, concentration of Cd(II) ions 25 mg L⁻¹ and shaking time 20 min at 25 °C. Different isotherms such as Langmuir, Freundlich and Dubinin-Radushkevich (D-R) isotherms fitted well to adsorption data with correlation coefficient (R²) of 0.998, 0.982 and 0.992, respectively. Monolayered (Q_m) and multi-layered (K_F) capacities of CoAl-AAP-LDH for adsorption of Cd(II) ions were calculated and found to be 34.40 and 19.44 mg g⁻¹, respectively. Sorption energy was calculated and found to be 9.13 kJ mol⁻¹, indicating chemisorption or ion exchange sorption mechanism. The method worked well for the adsorption of Cd(II) ions from wastewater samples.

Keywords: Layered Double Hydroxides, Enolate ions, Intercalation, Adsorption, Cd(II) ions, Isotherms

Introduction

Layered double hydroxides (LDH) are two dimensional ionic lamellar compounds, also known as hydrotalcite-like or compounds. They are composed of divalent and trivalent metal ions hydroxides sheets/layers possessing a positive charge. The positive charge on sheets/layers is due to the substitution of some portion of M²⁺ cation of the brucite-like layer with M³⁺ [1,2]. These sheets are sandwiched, intercalated with anions for balancing the positive charge. LDH is represented by

general formula [M_{1-x}²⁺M_x³⁺(OH)₂]^{x+}(A_{x/n}ⁿ⁻)^{x-}·yH₂O, where M²⁺ is divalent cations such as Mg, Co, Zn, Ni, Cd, Mn, etc., M³⁺ is trivalent cations such as Al, Fe, Cr, Ga, Bi, etc. in the brucite-like layers and Aⁿ⁻ is intercalated anions possessing n charge such as CO₃²⁻, NO₃⁻, OH and Cl⁻, x is equal to the molar ratio of M²⁺/(M²⁺ + M³⁺), n can be in the range of 0.2–0.33, and y is the number of water molecules [3]. Various LDHs have been synthesized by coprecipitation of mixed metal

cations ($M^{2+} + M^{3+}$) solution using NaOH base and urea as a source of a base at different conditions such as composition ratio of $M^{2+} + M^{3+}$ solution, temperature and aging period. The anions can be deintercalated or converted to mixed oxides by calcination. Taking the advantage of memory effect, various LDHs have been prepared mixed oxides by reconstruction approach followed by hydrolysis [4]. Due to anion exchangeability, compositional flexibility, biocompatibility, LDHs have been attracted for various applications as catalysts or catalyst precursors, flame retardants, stabilizers for polymers, and electroactive, photoactive materials, anion exchangers, adsorbent, etc. [5]. The selectivity and efficiency of the LDH adsorbent can be improved by acid activation, surface modification and thermal treatment, and intercalation of inorganic and organic anions [6]. Intercalated anions are exchangeable with suitable inorganic and organic anions, due to which LDHs have been attracted as selective and efficient adsorbents [7]. Various organic anions such as ethylenediaminetetraacetate (EDTA) [8,9], mercaptocarboxylic acid in to MgAl [10], aurintricarboxylic acid [11], amino acids [2,12], Chromotropic acid [13], Schiff base [14], diethylenetriamine-pentaacetic acid [15], diethylenetriamine-pentaacetate, meso-2,3-dimercaptosuccinate [16], citrate, malate and tartrate [17] have been interacted into LDH for the adsorption metal ions. To the best of our knowledge, there is no report on enolate intercalation into LDH. In the present study, enolate of 4-Aminoacetophenone (AAP) will be intercalated into CoAl-LDH for Cd(II) ions adsorption from aqueous samples.

Materials and Methods

Perkin Elmer flame atomic absorption spectrometer (AAnalyst 800, USA) with hollow cathode lamp was employed for Cd(II) ions determination. Thermo Scientific FT-IR

spectrometer (Nicolet iS10, UK) was used to record the FT-IR spectrum. The material was characterized by powder X-ray diffraction (XRD) by Diffractometer (Bruker D8 advance, German) employing Cu-K α ($\lambda=1.54056 \text{ \AA}$). Samples were scanned in the range of $2\theta = 5.0^\circ-80^\circ$ at 0.01° intervals at room temperature. A scanning electron microscope (JSM-6490LV, JEOL, Japan) was used for scanning SEM images. Bruker X-Flash 4010 133ev (made in Germany) using Cu-K α ($\lambda = 1.5406 \text{ \AA}$) radiation was used for EDX analysis. Shaker (Model No.1-4000, Germany) was used for shaking purpose. For pH measurements, a pH meter (inoLab pH 720, Germany) was used. Double distilled water and analytical reagent grade chemicals were used throughout the research. $\text{Co}(\text{NO}_3)_2 \cdot 6\text{H}_2\text{O}$, $\text{Al}(\text{NO}_3)_3 \cdot 9\text{H}_2\text{O}$ were purchased from Sigma-Aldrich, China. $\text{CH}_3\text{COOH}/\text{CH}_3\text{COONa}$, $\text{H}_3\text{PO}_4/\text{NaH}_2\text{PO}_4$ and $\text{NH}_4\text{OH}/\text{NH}_4\text{Cl}$ were used as buffer solutions for maintaining the desired pH.

Preparation of CoAl-NO₃ LDH

CoAl-NO₃ LDH was prepared, followed by co-precipitation method [9,18,19]. Experimentally, an aqueous 0.1 mol L⁻¹ NaOH solution was prepared and added dropwise to 500 mL of an aqueous solution containing 0.03 mol of $\text{Co}(\text{NO}_3)_2 \cdot 6\text{H}_2\text{O}$ and 0.01 mol of $\text{Al}(\text{NO}_3)_3 \cdot 9\text{H}_2\text{O}$ with stirring continuously until pH reached 10. The mixture was stirred continuously for 24 h at room temperature and the resulting slurry was aged at room temperature for 124 h and centrifuged. The final precipitated product (CoAl-NO₃-LDH) was filtered and washed with water until filtrate turned to neutral and oven-dried at 60 °C for 24 h.

Intercalation of AAP into CoAl-NO₃-LDH

Figure 1 shows the scheme for intercalation of enolate ions into CoAl-NO₃-LDH followed by the reconstruction approach

[20-22]. Experimentally, nitrate ions were deintercalated from CoAl-NO₃-LDH by calcination at 400 °C in the furnace. Thereafter, 1.5 g of AAP was tautomerized by dissolving in 100 mL of methanol, containing 0.01 g of NaOH. Thereafter, 1.0 g of calcined material was dispersed in the solution and refluxed for 4 h. The final product (CoAl-AAP-LDH) was filtered, washed with water until filtrate turned neutral and oven-dried at 60 °C for 24 h.

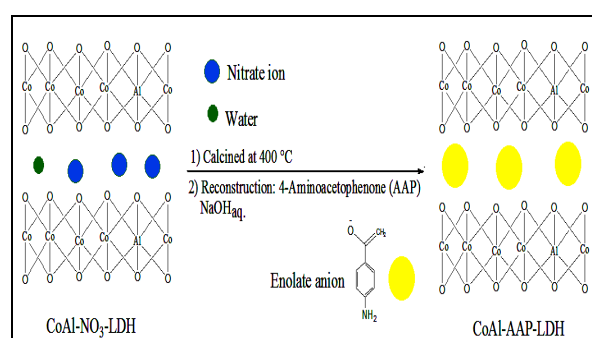


Figure 1. Scheme for intercalation of enolate ions into CoAl-NO₃-LDH

Adsorption Experiment

The efficiency of CoAl-AAP-LDH adsorbent for the adsorption of Cd(II) ions was tested by the batch procedure. Experimentally, 25 mg of CoAl-AAP-LDH adsorbent was placed into 100 mL bottle containing 20 mL of 25 mg L⁻¹ Cd(II) ions of pH 7.0 and shaken at 120 rpm for 20 min at room temperature. The mixture was filtered and filtrate was subjected to FAAS for determination of residual Cd(II) ions. The adsorption of Cd(II) ions was 95.5%, as calculated by equation 1.

$$\text{Adsorption (\%)} = \frac{[C]_i - F_f}{C_1} \times 100 \quad (1)$$

Where C_i and C_f are the initial and final concentrations of Cd(II) ions, respectively.

Results and Discussions

Characterization

FT-IR spectroscopy

Figure 2 shows FT-IR spectra of CoAl-NO₃-LDH (a), calcined CoAl-LDH (b) and CoAl-AAP-LDH (c). Peaks in spectrum-a at 3377.69 cm⁻¹ correspond to stretching vibrations of O-H bonds of LDH sheet and intercalated water [23], peak at 1646.56 cm⁻¹ attributed to bending vibration of O-H bond of intercalated water [9], peak at 1346.49 cm⁻¹ corresponds to stretching vibration of N=O bond of intercalated nitrate ions [24, 25] and peak at 844.48 cm⁻¹ attributed to stretching vibrations of M-O (Co-O and Al-O) bond of metal hydroxides, respectively [22]. This spectral information indicated the intercalation of nitrate ions and water into the CoAl-LDH. The broad weak peak in spectrum-b at 3377.69 cm⁻¹ attributed to stretching vibrations of O-H bonds of LDH sheet and intercalated residual water, weak peak at 1646.56 cm⁻¹ attributed to the bending vibration of O-H bond of water, which was probably captured from environment. The peak at 844.48 cm⁻¹ attributed to the stretching vibrations of M-O bonds of metal hydroxides. The absence of a signal at 1346.49 cm⁻¹ confirmed the deintercalation of nitrate ions. The broad weak peak in spectrum-c at 3288.06 cm⁻¹ attributed to stretching vibrations of O-H bonds of LDH sheet and intercalated residual water and weak peak at 1646.38 cm⁻¹ attributed to the bending vibration of O-H bond of residual water. The additional characteristic peaks in spectrum-c at 1556.5, 1442.49 and 1442.49 cm⁻¹ attributed to the stretching vibrations of C=C bonds of enolate ions of AAP. Peak at 844.48 cm⁻¹ correspond to M-O bonds of metal hydroxides, which indicated the formation of CoAl-AAP-LDH.

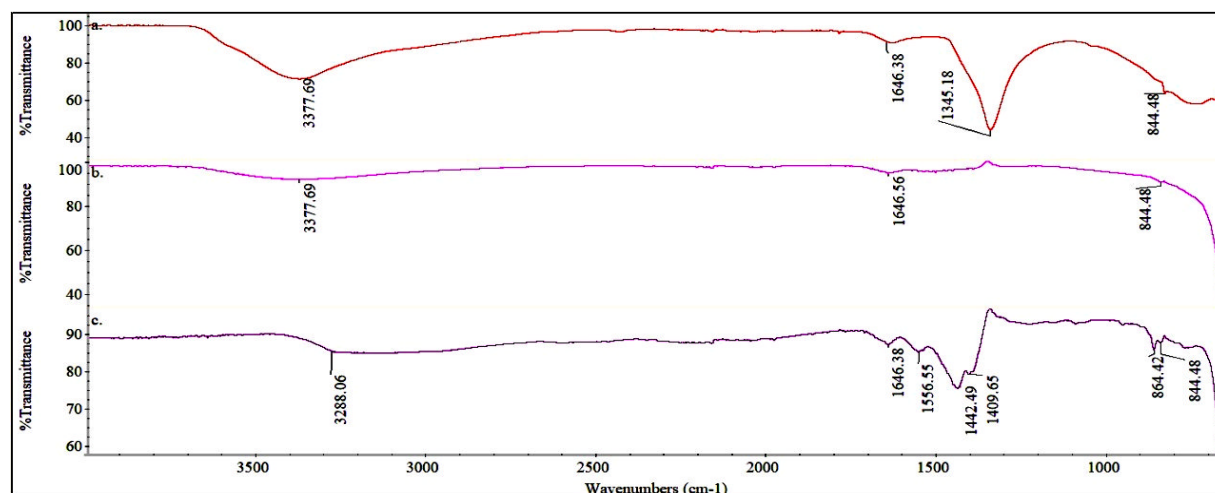


Figure 2. FT-IR spectra: CoAl-NO₃-LDH (a), calcined CoAl-LDH (b) and CoAl-AAP-LDH (c)

XRD

Fig. 3 shows the powder XRD pattern of CoAl-NO₃-LDH (a) and CuAl-AAP-LDH (b). The characteristic diffraction peaks in XRD pattern (a) at 2θ values 11.57°, 23.53°, 34.42°, 60.257° and 61.609° correspond to (003) and (006), (012), (110) and (113) planes (*hkl*) of hexagonal CoAl-NO₃-LDH phase, respectively, which confirmed the formation of hydrotalcite-like structured CoAl-NO₃-LDH [26]. According to Bragg's law ($d = n\lambda/2\sin\theta$, where λ is the wavelength of X-rays (for Cu K α , $\lambda = 1.54056 \text{ \AA}$) and $n=1$ (order of diffraction) and θ is the position of peaks in radian) [24], the d_{006} (basal spacing) in CoAl-NO₃-LDH was found to be 0.76 nm, which indicated the intercalation of water molecules and nitrate anions between hydrotalcite-like layers. Using the Debye Scherrer equation [27], the average crystallite size of CoAl-NO₃-LDH was calculated and found to be 199.04 nm. The characteristic diffraction peaks in XRD pattern (b) at 2θ values 11.38°, 22.85°, 34.42°, 60.36° and 61.69° correspond to (003) and (006), (012), (110) and (113) planes of hexagonal CoAl-AAP-LDH phase, respectively, which confirmed the reconstruction of hydrotalcite-like layers [20-22] and d_{006} was increased to 0.78 nm, which

indicated the intercalation of enolate anions of AAP between hydrotalcite-like layers. The broadness in the peaks is due to a decrease in crystalline size.

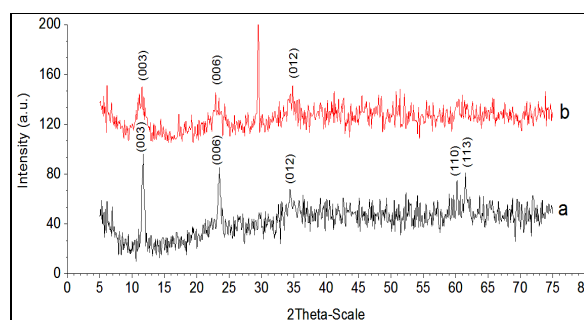


Figure 3. XRD patterns: CoAl-NO₃-LDH (a) and CuAl-AAP-LDH (b)

SEM analysis

Fig. 4 shows SEM Images of CoAl-NO₃-LDH (a), calcined LDH (b) and CoAl-AAP-LDH (c). By comparing images a and b, the characteristic change in morphologies can be seen, which indicated deintercalation of nitrate ions and formation of mixed CoAl oxides, occurred by calcination at 400 °C. By comparing images b and c, the characteristic changes in morphologies can be seen, which confirmed the reconstruction of LDH by intercalation of AAP i.e., CoAl-AAP-LDH.

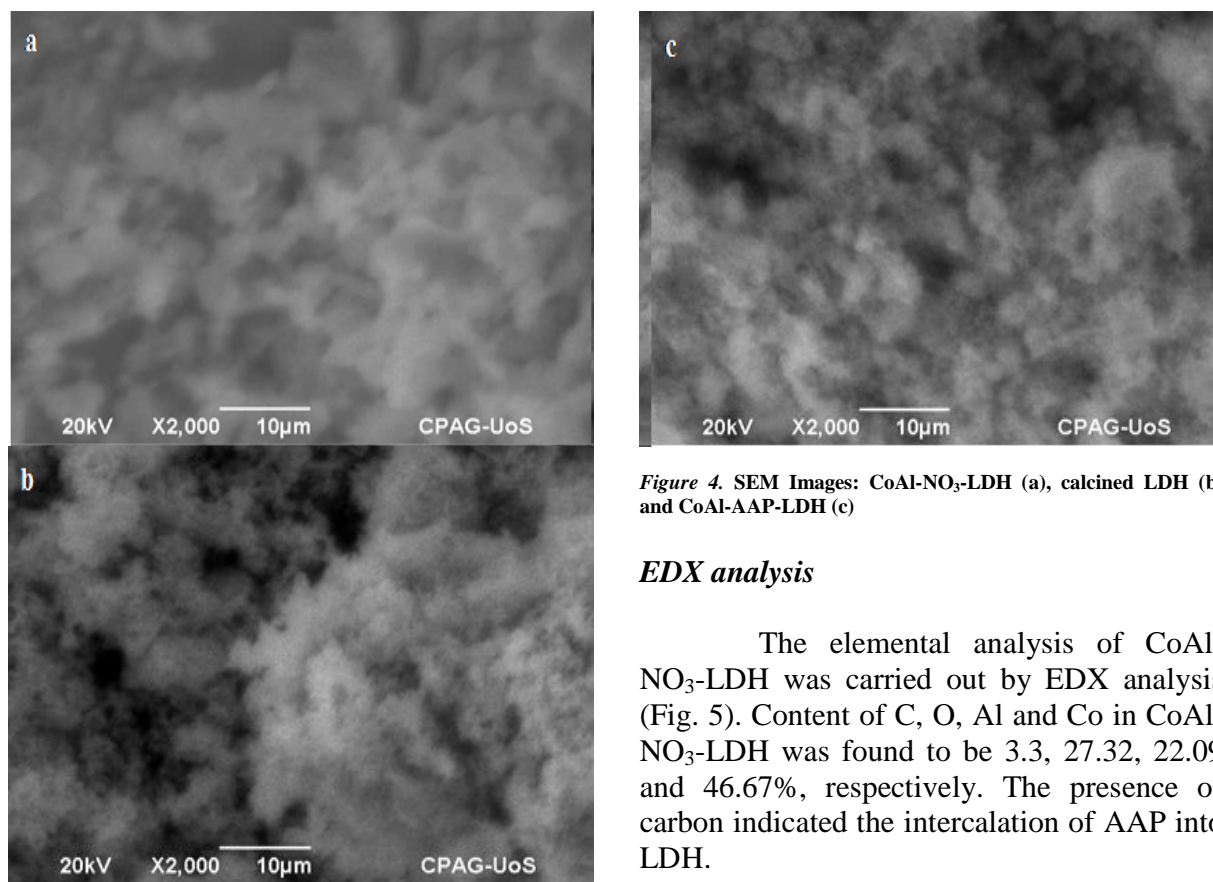


Figure 4. SEM Images: CoAl-NO₃-LDH (a), calcined LDH (b) and CoAl-AAP-LDH (c)

EDX analysis

The elemental analysis of CoAl-NO₃-LDH was carried out by EDX analysis (Fig. 5). Content of C, O, Al and Co in CoAl-NO₃-LDH was found to be 3.3, 27.32, 22.09 and 46.67%, respectively. The presence of carbon indicated the intercalation of AAP into LDH.

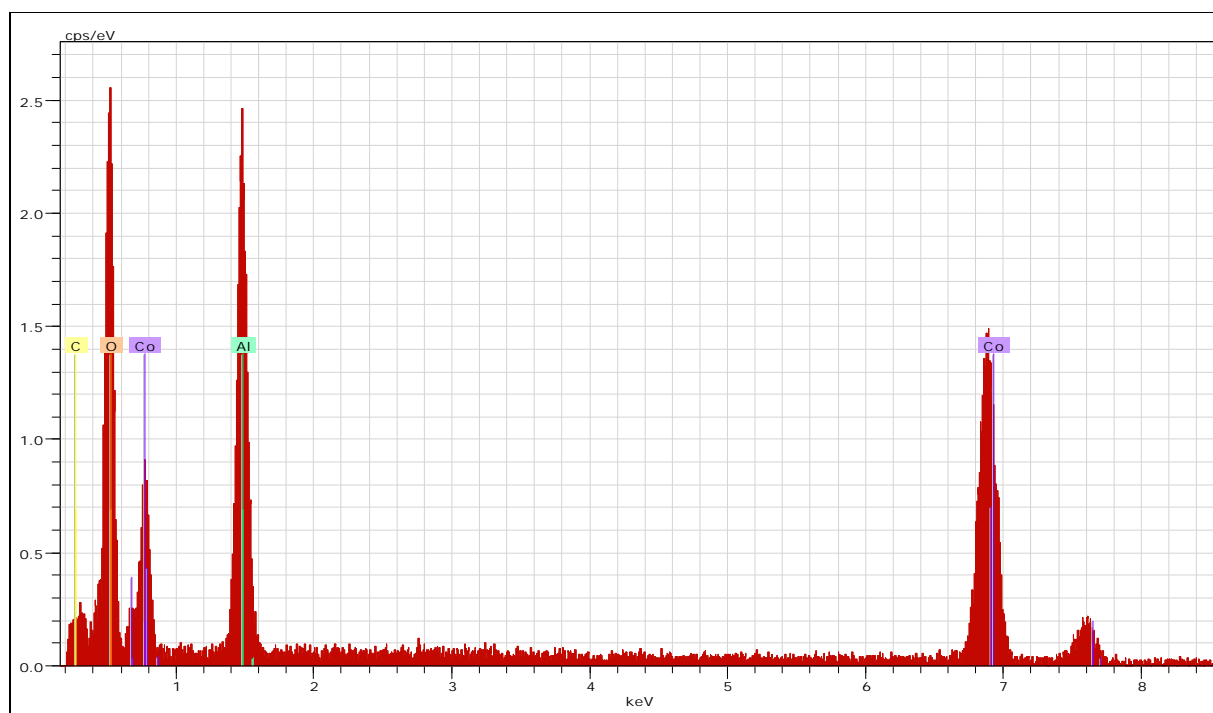


Figure 5. EDX of CoAl-AAP-LDH

Optimization

Effect of pH

The effect of pH 2-9 on adsorption of Cd(II) ions onto CoAL-AAP-LDH was examined. Cd(II) ions were adsorbed 94.0% at pH 7, as shown in Fig. 6a. The adsorption trend can be justified as in an acidic medium, Cd²⁺ ions and H⁺ ions were competing for interacting with CoAL-AAP-LDH adsorbent, While, with increasing of pH 4-7, H⁺ ions were decreasing and Cd(II) ions were interacted dominantly, resulted increase in adsorption. Further increasing of pH 8-9, adsorption was increased, which is due to the formation of Cd(OH)₂ precipitates [28,29]. Therefore, pH 7 was chosen as the optimum pH for further experiments.

Effect of shaking time

Adsorption depends on the contact time between adsorbent and adsorbate. Practically, the effect of contact time 5-50 min on Cd(II) ions adsorption onto CoAL-AAP-LDH adsorbent was studied. Adsorption of Cd(II) ions was increased with the increase of contact time and became maximum at 20 min (Fig. 6b). The adsorption was slightly decreased with further increasing of shaking time due to desorption. Therefore, 20 min was chosen as the optimum shaking time for further experiments.

Effect of adsorbent dosage

Different dosage 5-50 mg of CoAL-AAP-LDH adsorbent for the adsorption of Cd(II) ions was tested. The adsorption was increased with increasing of adsorbent dosage and reached to maximum at 30 mg as depicted in Fig. 6c. Adsorption was slightly decreased and then became almost constant with further increase of the dosage 30-50 mg. Therefore, 25 mg of the adsorbent was chosen as the best dose for further adsorption experiments.

Effect of concentration

The concentration of adsorbate is an important parameter that shows the uptake efficiency of adsorbent. Thus, the effect of initial concentration ranging 5-50 mg L⁻¹ of Cd(II) ions was examined as shown in Fig. 6d. The adsorption was increased with increasing of concentration ranging 5-25 mg L⁻¹ of Cd(II) ions and slightly decreased with further increasing of concentration due to fully saturation at the surface of CoAL-AAP-LDH. Therefore, the optimum concentration of Cd(II) ions was chosen as 25 mg L⁻¹ for further experiments.

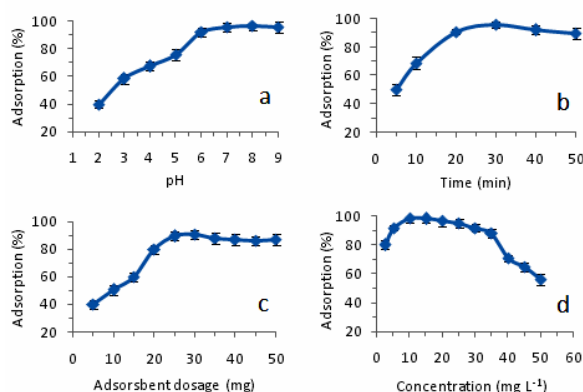


Figure 6. Optimization: Effect of pH (a), shaking time (b), dosage (c) and concentration (d)

Effect of matrix ions

The performance of adsorbent for adsorption of Cd(II) ions was assessed in the presence of 500 mg L⁻¹ various common ions such as Na⁺, K⁺, Mg²⁺, Ca²⁺, Cl⁻, F⁻, HCO₃⁻, CO₃²⁻, SO₄²⁻, NO₃⁻ and CH₃COO⁻. Therefore, adsorbent worked well and ≥90.5% of Cd(II) ions was adsorbed onto the adsorbent.

Equilibrium Studies

Equilibrium study for the adsorption of Cd(II) ions onto LDH was carried at room temperature by varying the concentration of

Cd(II) ions in the range of 5-50 mg L⁻¹ while other parameters were fixed at their optimum levels i.e., adsorbent dosage = 25 mg, pH = 7.0 and shaking time = 20 min. Different isotherms such as Langmuir isotherm, D-R isotherm and Freundlich isotherms were plotted for analyzing the adsorption data.

Langmuir isotherm

Langmuir isotherm assumes that the surface of adsorbent is homogeneous, possessing equally distributed active sites for adsorption. All the active sites have equal affinity for adsorption with constant adsorption energy. Monolayered sorption occurs onto the surface of adsorbent without interaction between adsorbed molecules or metal ions. A linear form of Langmuir isotherm is represented by equation 2.

$$\frac{C_e}{C_{ads.}} = \frac{1}{Q_m} C_e + \frac{1}{Q_m b_L} \quad (2)$$

Where C_e (mg L⁻¹) is the concentration of Cd(II) ions in the aqueous phase at equilibrium, $C_{ads.}$ (mg g⁻¹) is the amount of Cd(II) ions adsorbed onto the surface of adsorbent. Where Q_m (mg/g⁻¹) is the maximum adsorption capacity (mono layered) of the adsorbent and b_L (L mg⁻¹) is Langmuir constant, related to the affinity of active sites for adsorption and binding energy. The characteristic of Langmuir isotherm is the separation factor (R_L) which can be calculated by equation 3. The values of R_L suggest the feasibility of adsorption. The adsorption may be irreversible ($R_L = 0$), unfavorable ($R_L > 1$), and favorable ($0 < R_L < 1$) [30].

$$R_L = \frac{1}{1 + (b_L C_1)} \quad (3)$$

The Langmuir isotherm was plotted (Fig. 7) as $C_e/C_{ads.}$ versus C_e and fitted well to adsorption data with $y = 0.029x + 0.020$, $R^2 = 0.998$. The monolayered sorption capacity

of CoAl-AAP-LDH adsorbent for Cd(II) ions was calculated and found to be 34.40 mg g⁻¹. Values of R_L were calculated and found to be in the range of 0.064-0.02, suggested that adsorption of Cd(II) ions onto CoAl-AAP-LDH adsorbent was favorable.

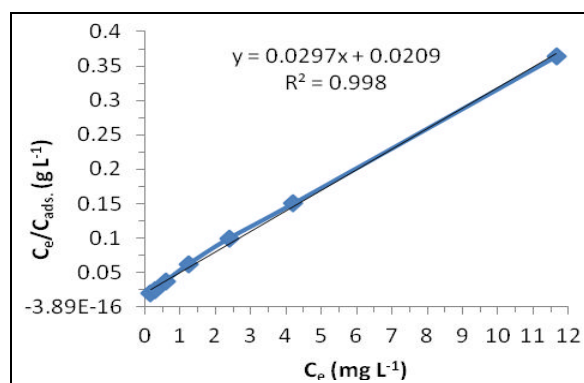


Figure 7. Langmuir isotherm

Freundlich isotherm

Freundlich isotherm describes multi-layered adsorption onto the surface of adsorbent by assuming that the surface of adsorbent is heterogeneous, possessing different (unequal) active sites. The sites possess a different affinity for adsorption with different sorption energy. The linear form of Freundlich isotherm is represented by equation 4 [31].

$$\text{Log } c = C_{ads.} = \frac{1}{n} \text{Log } C_e + \text{Log } K_F \quad (4)$$

Where K_F is the Freundlich constant and related to the maximum adsorption capacity of metal ions (mg g⁻¹) and $1/n$ is a dimensionless constant which illustrates the adsorption intensity. The Freundlich isotherm was plotted (Fig. 8) as $\text{Log } C_{ads.}$ versus $\text{Log } C_e$ and fitted well to adsorption data with $y = 0.225x + 1.288$, $R^2 = 0.981$. Multi-layered sorption capacity of adsorbent for Cd(II) ions was calculated and found to be 19.44 mg g⁻¹ with $1/n$ of 0.225, which suggested that active

sites are heterogeneously distributed onto the surface of adsorbent.

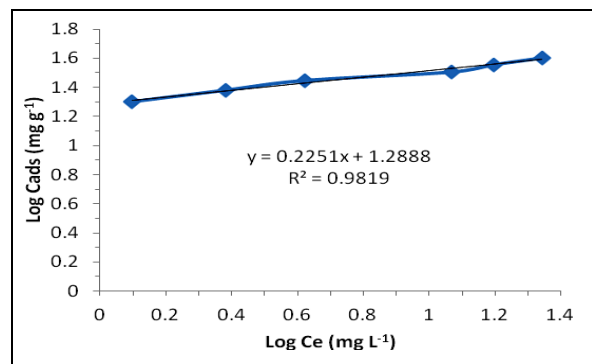


Figure 8. Freundlich isotherm

D-R isotherm

The D-R isotherm assumes no homogeneous surface of adsorbent. It is useful to estimate the characteristics of porosity of the adsorbent and energy of adsorption. A linear form of D-R isotherm is represented by equation 5.

$$\ln C_{\text{ads}} = \ln K_{\text{D-R}} - \beta \varepsilon^2 \quad (5)$$

Where β is the slope of D-R isotherm, $K_{\text{D-R}}$ is D-R constant and ε is polanyi potential, which can be calculated by equation 6.

$$\varepsilon = RT \ln \left(1 + \frac{1}{C_e} \right) \quad (6)$$

Where R (general gas constant) = $8.314 \text{ J mol}^{-1} \text{ K}^{-1}$ and T is temperature = 298 K and E is Free energy of adsorption can be calculated by equation 7. Value of E predicts the mechanism of adsorption, which can be physisorption if $E < 8 \text{ kJ mol}^{-1}$ or chemisorption if $E > 8-16 \text{ kJ mol}^{-1}$ [30]. The D-R isotherm was plotted (Fig. 9) as $\ln C_{\text{ads}}$ versus ε^2 and fitted well with $y = -0.006x - 0.9742$, $R^2 = 0.9917$. E was calculated and found to be 9.13 kJ mol^{-1} , suggested

chemisorptions or/and ion exchange mechanism of for adsorption of Cd(II) ions onto CoAl-AAP-LDH.

$$E = \frac{1}{\sqrt{-2\beta}} \quad (7)$$

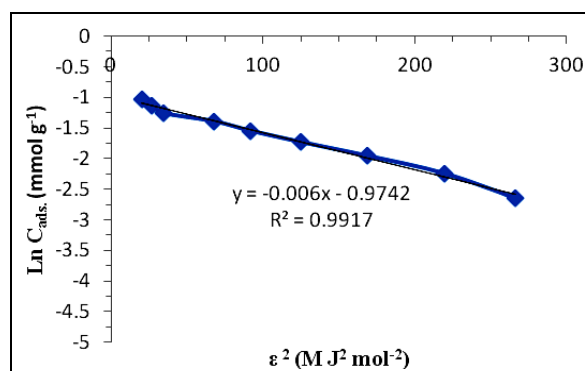


Figure 9. D-R isotherm

Application of the method

The repeatability of the developed method was checked by applying on spiked water samples. Removal of Cd(II) ions achieved was $>94.0\%$ as shown in Table 1. The results showed that Cd(II) ions were removed from spiked water samples.

Table 1. Application of method: Removal of Cd(II) ions from spiked wastewater samples.

Samples	Added (mg L ⁻¹)	Found (mg L ⁻¹)	Removal (%)±RSD
S-I	0.0	ND	-
	5.0	4.5	90.0±4.0
	10	9.5	95.0±3.0
	20	18.6	93.0±3.0
S-II	0.0	ND	-
	5.0	4.1	82.0±4.0
	10	9.2	92.0±3.5
	20	17.9	89.5±4.0

ND: Not detected; S-I: Tap water sample collected from research laboratory, Institute of Chemistry, University of Sindh Jamshoro, Pakistan; S-II Wastewater sample collection from Combined Effluent Treatment Plant in Korangi, Karachi, Pakistan

Comparison with Reported Methods

Various LDH adsorbents have methods synthesized for adsorption of Cd(II) ions from aqueous samples. The capacity of CoAl-AAP-LDH is comparatively better than reported adsorbents, as shown in Table 2.

Table 2. Comparative capacities of LDHs adsorbents for adsorption of Cd(II) ions.

Adsorbents	Q _m (mg g ⁻¹)	pH	Ref.
MgAl-Humate	39.34	5.0	[32]
MgAl-Cl	52.38	5.0	[33]
Fe ₃ O ₄ /MgAl-LDH	45.64	4.0	[34]
MgAl-LDH	61.38	9.0	[34]
NiAl-LDH	10.70	7.0	[35]
Carbon quantum dots/ZnAl-LDH	12.60	6.0	[36]
NiMo-LDH	53.60	5.5	[37]
Maifanite/MgAl-LDHs	3.77	7.0	[38]
ZnAl-EDT-LDH/ Poly(vinyl alcohol)	9.54	5.0	[39]
MgMn-LDH	633.44	5.0	[40]
Kiwi-biocha/MgFe LDH	25.60	5.5	[41]
Heat treated humic acid/MgAl-LDH	155.28	7.0	[42]
CoAl-AAP-LDH	34.40	7.0	This work

Conclusion

CoAl-NO₃-LDH was synthesized by co-precipitation method. The precipitated product was aged for a period of 120 for enhancing the crystalline size. The formation of layered material was confirmed from XRD pattern by showing an intense peak at $2\theta = 11.57^\circ$ and 23.53° . The basal spacing (d_{006}) in CoAL-NO₃-LDH was found to be 0.76 nm, which indicated the intercalation of nitrate anions and the average crystallite size of CoA-NO₃-LDH was calculated and found to be 199.04 nm. The nitrate anions were deintercalated by calcined at 400 °C, and enolate ions were intercalated into LDH by reconstruction approached. Different

isotherms such as Langmuir, Freundlich and D-R isotherms fitted well to adsorption data with R² of 0.992-0.982. Q_m and K_f of CoAl-AAP-LDH adsorbent for adsorption Cd(II) ions were calculated and found to be 34.40 and 19.44 mg g⁻¹, respectively. Sorption energy was found to be 9.13 kJ mol⁻¹, which indicated that Cd(II) ions was adsorbed onto the CoAl-AAP-LDH adsorbent by chemisorption or and ion exchange mechanism. The CoAl-AAP-LDH adsorbent has high efficiency for Cd(II) ions. The Adsorbent was recycled 20 times with a significant declining its performance.

Acknowledgment

The authors would like to thank Professor Dr. Saima Qayoom Memon for her scientific guidance.

Conflicts of Interest

The authors declare that there is no conflict of interest.

References

1. H. Shu, Z. Guan-Nan, Z. Chao, W. T. Weng, X. Yong-Yao and L. Tianxi, *ACS Appl. Mater. Interf.*, 4 (2012) 2242. doi.org/10.1021/am300247x.
2. T. Hibino, *Chem. Mater.*, 16 (2004) 5482. doi.org/10.1021/cm048842a.
3. P. Tang, F. Deng, Y. Feng and D. Li, *Ind. Eng. Chem. Res.*, 51 (2012) 10542. doi.org/10.1021/ie300645b.
4. X. Qiu, K. Sasaki, S. Xu and J. Zhao, *Langmuir*, 35 (2019) 6267. doi.org/10.1021/acs.langmuir.8b04196.
5. Y. Yang, X. Zhao, Y. Zhu and F. Zhang, *Chem. Mater.*, 24 (2011) 81. doi.org/10.1021/cm201936b.

6. M. Zubair, M. D and G. McKay, F. Shehzad and M. A. Al-Harhi, *Appl. Clay Sci.*, 143 (2017) 279. doi.org/10.1016/j.clay.2017.04.002.
7. M. Rosset, L. W. Sfreddo, O. W. Perez-Lopez and L. A. Féris, *J. Environ. Chem. Eng.*, 8 (2020) 103991. doi.org/10.1016/j.jece.2020.103991.
8. K. A. Tarasov, D. O. Hare and V. P. Isupov, *Inorg. Chem.*, 42 (2003) 1919. doi.org/10.1021/ic0203926.
9. M. R. Perez, I. Pavlovic, C. Barriga, J. Cornejo, M. C. Hermosín and M. A. Ulibarri, *Appl. Clay Sci.*, 32 (2006) 245. doi.org/10.1016/j.clay.2006.01.008.
10. H. Nakayama, S. Hiramí and M. Tshuhako, *J. Colloid. Interf. Sci.*, 315 (2007) 177. doi.org/10.1016/j.jcis.2007.06.036.
11. H. Zhu, Y. Feng, P. Tang, G. Cui, D. G. Evans, D. Li and X. Duan, *Ind. Eng. Chem. Res.*, 50 (2011) 13299. doi.org/10.1021/ie2016366.
12. S. Aisawa, S. Takahashi, W. Ogasawara, Y. Umetsu and E. Narita, *J. Solid State Chem.*, 162 (2001) 52. doi.org/10.1006/jssc.2001.9340.
13. Y. Chen and S. Yu-Fei, *Ind. Eng. Chem. Res.*, 52 (2013) 4436. doi.org/10.1021/ie400108t.
14. N. Senda, I. Fujiwara and Y. Murakami, *Appl. Clay Sci.*, 183 (2019) 105310. doi.org/10.1016/j.clay.2019.105310.
15. X. Liang, W. Hou, Y. Xu, G. Sun, L. Wang, Y. Sun and X. Qin, *Colloids Surf. A*, 366 (2010) 50. doi.org/10.1016/j.colsurfa.2010.05.012.
16. I. Pavlovic, M. R. Perez, C. Barriga and M. A. Ulibarri, *Appl. Clay Sci.*, 43 (2009) 125. doi.org/10.1016/j.clay.2008.07.020.
17. T. Kameda, H. Takeuchi and T. Yoshioka, *Sep. Purif. Technol.*, 62 (2008) 330. doi.org/10.1016/j.seppur.2008.02.001.
18. S. V. Krishna and G. Pugazhenthí, *J. Exp. Nanosci.*, 8 (2013) 19. doi.org/10.1080/17458080.2011.551894.
19. K. Suresh, R. V. Kumar, R. Boro, M. Kumar and G. Pugazhenthí, *Mater. Today: Proceedings*, 5 (2018) 1359. doi.org/10.1016/j.matpr.2017.11.222.
20. T. Hibino and A. Tsunashima, *Chem. Mater.*, 10 (1998) 4055. doi.org/10.1021/cm980478q.
21. R. P. Bontchev, S. Liu, J. L. Krumhansl, J. Voigt and T. M. Nenoff, *Chem. Mater.*, 15 (2003) 3669. doi.org/10.1021/cm034231r.
22. H. Nakayama, N. Wada and M. Tshuhako, *Int. J. Pharm.*, 269 (2004) 469. doi.org/10.1016/j.ijpharm.2003.09.043.
23. F. R. Costa, A. Leuteritz, U. Wagenknecht, D. Jehnichen, L. Häußler and G. Heinrich, *Appl. Clay Sci.*, 38 (2008) 153. doi.org/10.1016/j.clay.2007.03.006.
24. W. Li, A. Liu, H. Tian and D. Wang, *Colloid. Interf. Sci. Commun.*, 24 (2018) 18. doi.org/10.1016/j.colcom.2018.03.003.
25. L. Mingsheng, X. Shun, G. Qingyang, D. Zuoxing, L. Qinglong and Z. Zhijun, *Colloid. Interf. Sci.*, 538 (2019) 440. doi.org/10.1016/j.jcis.2018.12.006.
26. W. Hong, J. Wang, L. Niu, J. Sun, P. Gong and S. Yang, *J. Alloys Compd.*, 608 (2014) 297. doi.org/10.1016/j.jallcom.2014.04.131.
27. P. F. Fato, L. Da-Wei, Z. Li-Jun, Q. Kaipei and L. Yi-Tao, *ACS Omega*, 4 (2019) 7543. doi.org/10.1021/acsomega.9b00731.
28. I. D. Smiciklas, S. K. Milonjić, P. Pfenđt and S. Raicevic, *Sep. Purif.*, 18 (2000) 185. [doi.org/10.1016/S1383-5866\(99\)00066-0](https://doi.org/10.1016/S1383-5866(99)00066-0).
29. S. E. A. S. El-Deen, S. I. Moussa, Z. A. Mekawy, M. K. K. Shehata, S. A. Sadeek and H. H. Someda, *Radiochim. Acta*, 105 (2017) 43.

- doi.org/10.1515/ract-2016-2624.
30. S. Q. Memon, S. M. Hasany, M. I. Bhangar, M. Y. Khuhawar, *J. Colloid Interf. Sci.*, 291 (2005) 84.
doi.org/10.1016/j.jcis.2005.04.112.
31. D. Kundu, S. K. Mondal and T. Banerjee, *J. Chem. Eng. Data*, 64 (2019) 2601.
doi.org/10.1021/acs.jced.9b00088.
32. M. A. Gonzalez, I. Pavlovic, R. Rojas-Delgado and C. Barriga, *Chem. Eng. J.*, 254 (2014) 605.
doi.org/10.1016/j.cej.2014.05.132.
33. M. A. Gonzalez, I. Pavlovic and C. Barriga, *Chem. Eng. J.*, 269 (2015) 221.
doi.org/10.1016/j.cej.2015.01.094.
34. R. Shan, L. Yan, K. Yang, Y. Hao and B. Du, *J. Hazard. Mater.*, 299 (2015) 42.
doi.org/10.1016/j.jhazmat.2015.06.003.
35. O. Rahmanian, M. H. Maleki and M. Dinari, *J. Phys. Chem. Solids*, 110 (2017) 195.
doi.org/10.1016/j.jpcs.2017.06.018.
36. O. Rahmanian, M. Dinari and M. K. Abdolmaleki, *Appl. Surf. Sci.*, 428 (2018) 272.
doi.org/10.1016/j.apsusc.2017.09.152.
37. M. S. Mostafa and A. B. Al-Sayed, *Energy Sources Part A*, 41 (2018) 2257.
doi.org/10.1080/15567036.2018.1555629.
38. X. Zhang, Y. Dou, C. Gao, C. He, J. Gao, S. Zhao and L. Deng, *Sci. Total Environ.*, 685 (2019) 951.
doi.org/10.1016/j.scitotenv.2019.06.228.
39. M. Dinari, A. Haghighi and P. Asadi, *Appl. Clay Sci.*, 170 (2019) 21.
doi.org/10.1016/j.clay.2019.01.007.
40. M. Chen, P. Wu, Z. Huang, J. Liu, Y. Li, N. Zhu, Z. Dang and Y. Bi, *J. Environ. Manage.*, 246 (2019) 164.
doi.org/10.1016/j.jenvman.2019.06.002.
41. Y. Tan, X. Yin, C. Wang, H. Sun, A. Ma, G. Zhang and N. Wang, *Environ. Pollut. Bioavailab.*, 31 (2019) 189.
doi.org/10.1016/j.jcis.2018.10.066.
42. M. Shi, Z. Zhao, Y. Song, M. Xu, J. Li and L. Yao, *Appl. Clay Sci.*, 187 (2020) 105482.
doi.org/10.1016/j.clay.2020.105482.